Green Chemistry

Accepted Manuscript

This is an *Accepted Manuscript*, which has been through the Royal Society of Chemistry peer review process and has been accepted for publication.

Accepted Manuscripts are published online shortly after acceptance, before technical editing, formatting and proof reading. Using this free service, authors can make their results available to the community, in citable form, before we publish the edited article. We will replace this *Accepted Manuscript* with the edited and formatted *Advance Article* as soon as it is available.

You can find more information about *Accepted Manuscripts* in the Information for Authors.

Please note that technical editing may introduce minor changes to the text and/or graphics, which may alter content. The journal's standard Terms & Conditions and the Ethical guidelines still apply. In no event shall the Royal Society of Chemistry be held responsible for any errors or omissions in this *Accepted Manuscript* or any consequences arising from the use of any information it contains.

ROYAL SOCIETY OF CHEMISTRY

www.rsc.org/greenchem

This review addresses changes in the physical structure of heterogeneous catalysts used for biomass conversion carried out in aqueous phase with increasing severity.

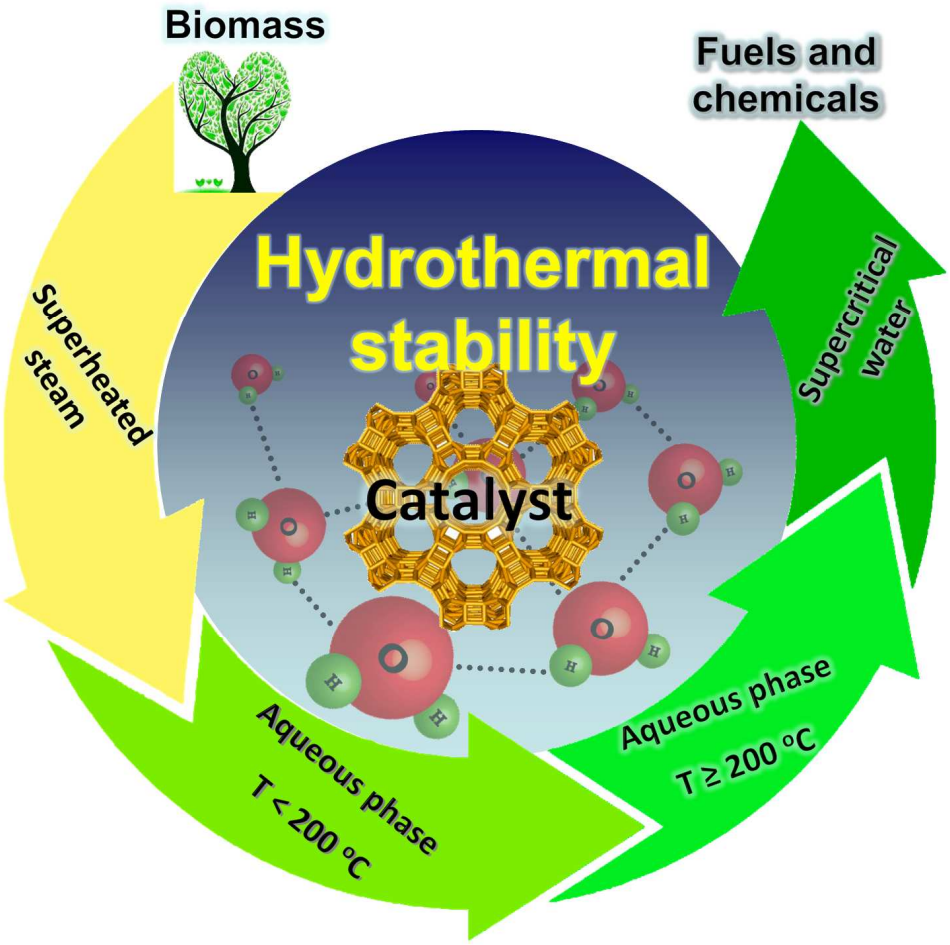

Green Chemistry Accepted Manuscript

Hydrothermally stable heterogeneous catalysts for conversion of biorenewables

Haifeng Xiong, Hien N. Pham and Abhaya K. Datye*

Center for Microengineered Materials and Department of Chemical & Biological Engineering, University of New Mexico, Albuquerque, New Mexico 87131, United States

* Corresponding author. Tel.: +1 505 277 0477; fax: +1 505 277 1024; Email: datye@unm.edu (A.K. Datye)

Abstract The catalytic conversion of biomass-derived molecules to fuels and chemicals involves reactions carried out in the aqueous phase. The corrosive effects of the reactive environment can cause degradation of heterogeneous catalysts, but the detrimental effects depend on the state of the water. For example, water vapor, superheated steam and sub- and supercritical liquid water can behave very differently. In this review, we focus on the hydrothermal stability of the heterogeneous catalysts in order of increasing severity of the reaction medium: superheated steam, liquid water at temperatures below 200 ^{o}C, liquid water at temperature above 200 ^{o}C and supercritical water. This review addresses changes in the physical structure of heterogeneous catalysts used for biomass conversion reactions. These physical changes influence catalytic performance, but other causes for deactivation include sintering of the metal phase or coking or carbon deposition on catalyst. The latter phenomena are not the primary focus of this review. We also describe recent approaches designed to improve the hydrothermal stability of heterogeneous catalysts in biomass conversion reactions.

1. Introduction

Biomass constitutes a sustainable feedstock for meeting our needs for fuels, chemicals and materials.[1] Because biomass-derived molecules are highly functionalized and water soluble, they are generally processed under aqueous phase conditions [1]. By processing biomass in the liquid phase, the energy costs for separation and purification can be avoided.

The conversion of biomass-derived molecules to fuels and chemicals involves reactions such as hydrolysis, dehydration, reforming, hydrogenolysis (C-C and C-O bonds), hydrogenation, aldol condensation, isomerization, selective oxidation, and water gas shift.[2] Fig. 1 shows the pressure-temperature phase diagram for pure water and the conditions where specific reactions are carried out during catalytic processing of biomass. As shown in Fig.1, hydrolysis, dehydration, isomerization, oxidation, aldol condensation, and hydrogenation are carried out at temperatures near or below 200 ^{o}C. Hydrogenolysis and hydrogenation reactions are usually carried out at higher temperatures (e.g. 200 ^{o}C), and reforming (gas and aqueous phases) is carried out at even higher temperatures (200-400 ^{o}C). To maintain the liquid phase, high pressures are necessary when operating above the boiling point of water.[2] At temperatures above 500 ^{o}C, homogeneous gasification and thermolysis can occur. Fig. 1 shows that biomass conversion reactions can be carried out in vapor, liquid and supercritical phases at temperatures from room temperature to 600 ^{o}C and pressures from atmospheric to 296.1 atm.

Green Chemistry Accepted Manuscript

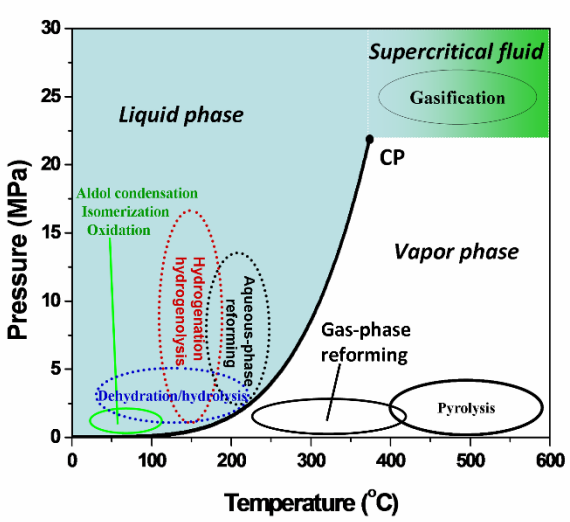

Fig. 1. Phase diagram for water indicating the temperature and pressure regimes for reactions of interest in the conversion of biomass derived molecules (CP-critical point).

Under these hydrothermal conditions, a key property for H_2O is the dissociation equilibrium of water (Eq. 1).

$$H_2O \rightleftharpoons H^+ + OH^- \qquad (1)$$

$$K_w = a(H^+)a(OH^-)$$

Where K_w is the ion product and *a* refers to the activity of each species. At normal conditions (room temperature and atmospheric pressure), $K_w = 1\times10^{-14}$, and the proton concentration equals the familiar value of 1×10^{-7} mol L^{-1} under neutral pH conditions. K_w increases with temperature and density.[3] For example, the ion product (K_w) increases from 10^{-14} at 25 °C to 10^{-11} just below 350 °C. This situation has dramatic consequences for hydrolysis and the acid-base equilibrium of water, which affects the reaction performance for liquid phase reactions. Enhanced corrosion is possible under these conditions for both the catalyst and the reactor.

Heterogeneous catalysts used in biomass conversion reactions are usually supported on porous materials having a high surface area, such Al_2O_3, SiO_2, TiO_2 and carbon. These materials are hydrophilic due to the existence of surface functionalities (proton, hydroxyl, carbonyl etc.), as shown in Fig. 2. These surface functional groups can be used to anchor active metals or metal oxides during catalyst preparation, or they can also act as catalysts for certain reactions. On the other hand, the H^+ and OH^{-1} ions can attack the surface of the porous supports and change the nature of the materials under severe hydrothermal conditions because the H^+ and OH^{-1} ion concentrations increase, therefore changing the catalytic performance of these materials. Although there are significant advances in the design of novel catalysts for the conversion of biomass, many of these catalysts do not possess adequate hydrothermal stability which can impact their long-term performance. Catalysts which are hydrothermally stable in vapor phase reactions may not be suitable for aqueous phase reactions. Furthermore, catalysts designed for use in biomass reactions at moderate temperatures (such as hydrogenation) may be unsuitable when used for reactions operated at higher temperatures (such as aqueous-phase reforming). Hence, it is necessary to develop strategies to modify heterogeneous catalysts to improve their stability when used for biomass conversion reactions.

Green Chemistry Accepted Manuscript

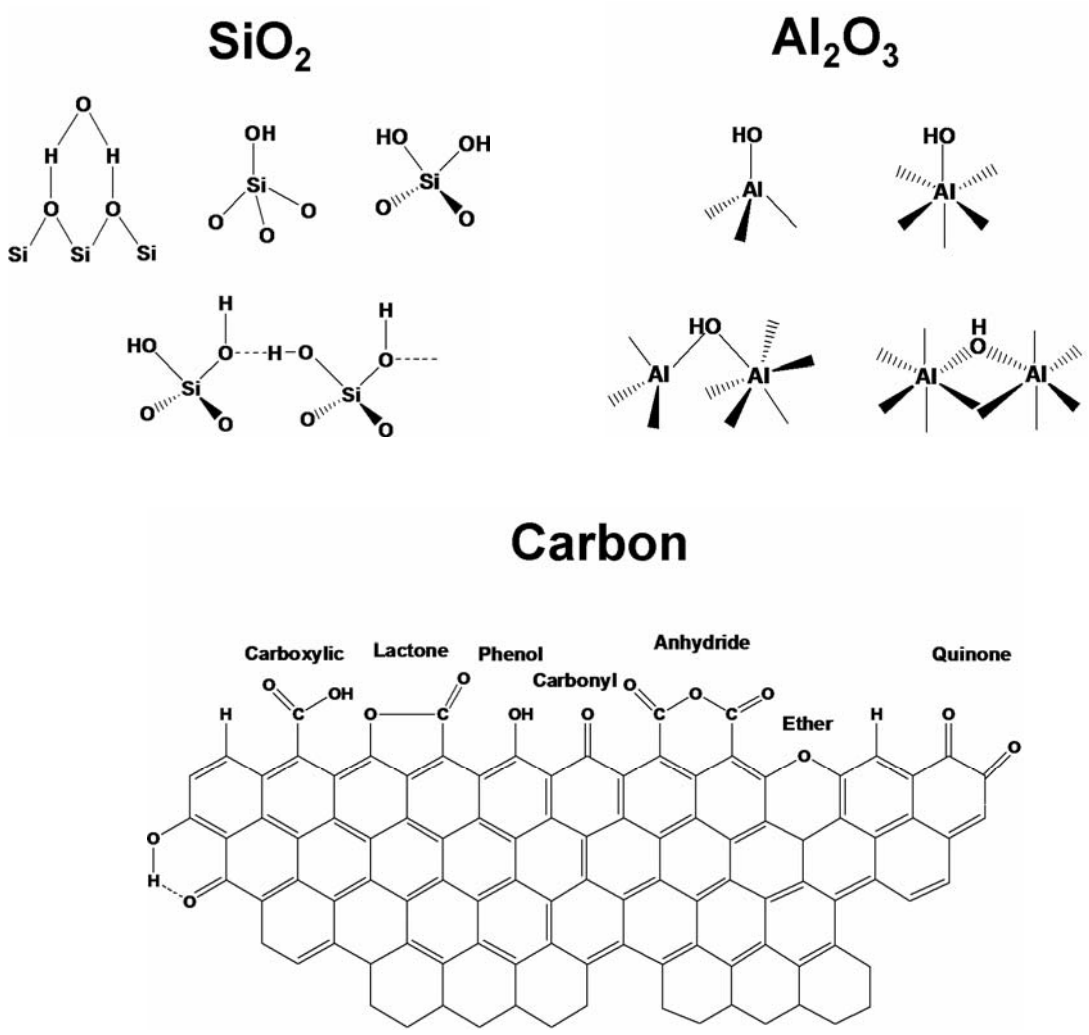

Fig. 2. Illustration of surface groups on SiO_2, Al_2O_3 and carbon based materials.

The purpose of this review is to describe recent developments in the synthesis and application of hydrothermally stable heterogeneous catalysts for biomass-derived reactions. We consider both vapor phase and aqueous phase conditions, and include our recent work on developing catalysts having improved hydrothermal stability. We also consider recent work on biomass conversion carried out in supercritical water. Two recent reviews have addressed engineering and thermodynamic aspects of working with water near the critical point.[3, 4] Our review focuses on the physical structure changes in heterogeneous catalysts used for biomass conversion reactions. The catalytic performance and catalyst deactivation resulting from sintering or coking are not included in the scope of this review since factors other than hydrothermal stability become significant. We characterize hydrothermal conditions that represent different degrees of severity[5] by organizing our review into four typical environments: super heated steam, liquid water below 200 ^{o}C, liquid water at temperature of above 200 ^{o}C and supercritical water above the critical point (T_c=373.95 ^{o}C, P_c=217.75 atm). We also address recent approaches developed to improve the hydrothermal stability of heterogeneous catalysts. In the last section of this review, we assess the state of the art and identify challenges for achieving catalyst stability in biomass conversion reactions.

Green Chemistry Accepted Manuscript

2. Hydrothermal conditions for biomass conversion reactions

2.1. Superheated steam

There is extensive literature on the study of hydrothermally stable heterogeneous catalysts under steam, in the petroleum industry as well as for automotive exhaust catalysis.[6, 7] Previous results have revealed that the hydrothermal stability of heterogeneous catalysts is closely associated with the conditions used (temperature, water content and aging time). Recently, porous silica- and alumina-based materials have been used as solid acid catalysts or supports for biomass conversion reactions such as dehydration, hydrolysis and reforming in superheated steam. This section focuses on the hydrothermal stability of commonly used oxide catalysts and supports for biomass conversion.

Silica-based materials The mostly common silica-based materials are amorphous silica (such as silica gel) and ordered mesoporous silica with uniform pore structure. In their study of hydrothermal stability, Kim and Ryoo concluded that the mesoporous structure of pure-silica framework MCM-41 was stable in 100% steam at 600 ^{o}C and 1 atm.[8] However, when MCM-41 was treated at 900 ^{o}C in a flow of nitrogen saturated with water vapor (treatment time was not reported), the surface area decreased from 943 to 131 m^2/g, indicating that MCM-41 was not hydrothermally stable at very high temperatures in steam.[9]

Another ordered mesoporous silica, SBA-15, has been used as a support in glycerol steam reforming (10 wt.% glycerol/water solution) at 500 and 650 ^{o}C.[10] It was demonstrated that after 20 h time-on-stream for the steam reforming reaction, SBA-15 possessed insufficient hydrothermal resistance because the SBA-15 mesostructure was gradually destroyed at both temperatures. This caused the progressive deactivation of the resulting Ni/SBA-15 catalyst. In another study, when SBA-15 was modified by small amounts of Nb (n_{Si}/n_{Nb}=10), hydrothermal treatment at 600 ^{o}C in steam (held for 12 or 24 h) caused some shrinkage of mesopores and structural disorder due to the small number of Si-O-Nb bonds.[11] However, when a higher amounts of tetrahedral Nb^{5+} species were incorporated into SBA-15 (n_{Si}/n_{Nb}=5), the NbSBA-15 kept its well-ordered mesoporous structure after a similar hydrothermal treatment, indicating that the higher loaded NbSBA-15 had superior hydrothermal stability.

The hydrothermal stability of a wide range of ordered mesoporous silica materials, including the molecular sieves MCM-41, MCM-48, HMS, FSM-16, KIT-1, PCH and SBA-15, has been compared by exposing the samples to a N_2 stream containing 30 vol% of water vapor at 400 ^{o}C for 48 and 120 h.[12] The results showed that these ordered silica materials retained their high surface area after this treatment. The hydrothermal stability was found to be influenced by the wall thickness and the degree of the silica polymerization and decreased according to the following trend: KIT-1 > SBA-15 > MCM-48, PCH > FSM-16, MCM-41, HMS.

Alumina-based materials Transitional alumina such as γ-Al_2O_3 and its related polymorphs are extensively used as catalysts and catalyst supports. However, the porous structure of these materials changes significantly when exposed to superheated steam.[13] The hydrothermal stability of alumina and aluminophosphate (AP) with Al/P ratio of 6 has been compared under treatment at 750 °C for up to 48 h.[14] The results indicate that AP had a higher hydrothermal stability than γ-alumina. The pore size distribution and surface area of AP did not change much under this hydrothermal condition, while the pore size distribution of alumina shifted toward larger pore diameters accompanied with decreasing surface area upon deactivation. The γ-alumina doped by La, Ni, Mn and Ga presented better hydrothermal stability than undoped γ-alumina [13, 15, 16].

Zeolites Zeolites are microporous aluminosilicates and composed of both Brønsted and Lewis acid sites. Thus, they are extensively used as solid acid catalysts for biomass conversion reactions. The stability of zeolites in steam has been reported to be related to the type of cation used, the Si/Al ratio and the framework configuration. The HZSM-5 catalyst having a high Si/Al ratio (SiO_2/Al_2O_3 = 80) has been used in the production of hydrocarbons from crude bio-oil derived from pyrolysis of lignocellulosic biomass.[17] The result showed that the HZSM-5 zeolite maintained its kinetic behavior for up to 10 reaction-regeneration cycles at 500 ^{o}C (~3 h time-on-

Green Chemistry Accepted Manuscript

stream each cycle) in steam, indicating this catalyst showed superior hydrothermal stability. The main reason for the stability was ascribed to the homogeneous, moderate acid strength and the low density of acid sites in the catalysts.[17] In contrast, a Cu-ZSM5 catalyst completely deactivated at 450-500 °C after 7 h under 2-2.5 vol% H_2O/He.[18] When a Cu-Beta zeolite catalyst was hydrothermally aged between 500 and 900 °C for 3 h in a stream of 8%O_2, 5%H_2O and 5%CO_2, a structural breakdown of the catalyst occurred at 900 °C and the surface area decreased from 550 to ca. 20 m^2/g.[19]

The effect of different Si/Al ratio on the hydrothermal stability of Ce^{3+} zeolite catalysts (Ce-ZSM-5, Ce-beta, Ce-mordenite and Ce-Y) have been investigated in a stream containing 10 or 12 % water vapor at 600 °C for 3-99 h.[20] The results showed that Ce-ZSM-5 (Si/Al ratios: Si/Al = 17.1, 22.6 and 146.6) and Ce-mordenite (Si/Al = 6.4, IE = 77.2%) showed fast deactivation. Ce-beta (Si/Al = 12, IE = 68.4%) and Ce-Y (Si/Al = 2.8, IE = 122%) were significantly more stable and showed high initial activities for selective catalytic reduction of NO_x. Ce-ZSM-5 showed an increase of non-framework Al, indicating that the zeolite suffered from dealumination.

The effect of catalyst particle size (0.2-0.9 μm) on the hydrothermal stability of the polycrystalline beta zeolites has been compared at 800 °C for 30 min in 10 mol% water vapor, in terms of changes in BET surface areas, crystallinity, and framework aluminum atoms.[21] It was found that the hydrothermal stability of beta zeolite increased with increasing particle size. The surface areas of beta zeolite with crystallite sizes in the range of 0.2-0.4 μm decreased significantly after hydrothermal treatment. The surface areas of beta zeolite with a particle size of 0.2 μm showed the highest loss of surface area (ca. 20%), while the beta zeolites with larger particle sizes ranging from 0.5-0.9 μm showed only 4-5% decrease in surface areas. The loss of surface area upon hydrothermal treatment suggested a partial collapse of the zeolite framework. However, hydrothermal treatment did not alter the relative crystallinity of beta zeolite, probably due to small amounts of Al atoms present in the unit cell of this zeolite.

Mixed oxide materials For the catalytic steam reforming of glycerol to allyl alcohol at 350 °C under atmospheric pressure, the addition of Al_2O_3 to a K/ZrO_2-FeO_x catalyst (K/Al_2O_3-ZrO_2-FeO_x) was found to be effective for achieving higher structural stability, leading to high glycerol conversion with stable allyl alcohol yield of above 25 mol% C.[22] The addition of heteroatoms also influences the hydrothermal stability of molecular sieves. The VPI-5 molecular sieve (aluminophosphate) contains extra-large pores (> 10 Å). When rapidly heated to 550 °C, VPI-5 can withstand exposure to humid helium (He bubbled through water) at the elevated temperatures with little loss of structural integrity. A microporous titanosilicate molecular sieve, ETS-10, consists of a 3D 12-ring structure.[23] The crystalline structure of ETS was seriously degraded in 100% steam at 600 °C for 2 h, while a ETS-10 molecular sieve modified with lanthanum retained a high crystallinity of 73% and possessed a large surface area of 260 m^2/g (initial surface area was 352 m^2/g), indicating a superior hydrothermal stability. Likewise, the hydrothermal stability of a paper-like ceramic fiber washcoated with V_2O_5/TiO_2 was investigated by treating the material at 700 °C for 12 h in a flow of 10%H_2O/air.[24] It was concluded that hydrothermal stability of the ceramic fiber improved due to the well-dispersed $AlPO_4$ formed on the substrate surface, which also inhibited the transformation of TiO_2 from the anatase to rutile phase.

The effect of hydrothermal aging under lean and lean/rich cycling conditions (containing 10 vol% H_2O) from 600 to 800 °C for 6 h on the physical properties of a commercial catalyst containing Pt/Pd/Rh, Ba, Ce, Zr, Mg, Al and various stabilizers has been investigated.[25] It was shown that the major impact of lean hydrothermal treatment on the catalyst was the continuous decrease of the specific surface area with aging temperature due to the collapse of smaller pores. The noble metal nanoparticles remained highly dispersed even after lean aging at 800 °C. In contrast, the noble metal sintering occurred due to lean/rich cycling, and there was a significant loss of crystallinity for the $BaCO_3$ component of the catalyst.

Nickel catalysts supported on titania, zirconia and a perovskite-type oxide $La_{1-x}Ca_xNiO_3$ have been used in glycerol steam reforming.[10, 26] For the titania and zirconia, no structure change

Green Chemistry Accepted Manuscript

was found when treated at high temperatures (500 or 650 °C) in 10 wt.% glycerol/water solution.[10] Likewise, the characterization result of spent $La_{1-x}Ca_xNiO_3$ catalyst (in a steam-to-carbon ratio of 3 at 550 °C upon 30 h) revealed that the smaller Ni particle size improved the catalyst stability.[26] However, when an aluminum borate with Al to B ratio of 10 was treated with water steam at 750 ° C for up to 48 h, the pore size distribution and the surface area of the aluminum borate changed.[27] This can be ascribed to the instability of the boron compounds.

In a summary, the stability of heterogeneous catalyst materials in superheated steam has been extensively investigated. These materials include zeolite-, silica- and alumina-based materials. The hydrothermal conditions and stability of heterogeneous catalysts in superheated steam is summarized in Table 1. Most studies were performed at T ≥ 400 °C and different water concentration and aging times. When treated at T < 400 °C in superheated steam, these materials demonstrated excellent stability. When these materials were processed at T ≥ 400 °C in steam, structure changes were found to take place. The extent of the structural change and the decrease of surface area were related to the factors such as the temperature, the water content and aging time. A simple illustration is shown in Fig. 3 and used to compare the relative stability of these materials under superheated steam conditions.

Table 1 Hydrothermal stability of heterogeneous catalysts in superheated steam

Catalyst	Composition (mol%)	Superheated steam			Structure change (Yes/No)	Ref.
		Temperature (°C)	Water vapor (v/v%)	Time (h)		
γ-Al_2O_3, α-Al_2O_3	pure	500	75	0-50	Y	13, 28
Ni-doped γ-Al_2O_3	0-10 Ni	500	75	0-50	N	28
Ce-, La-doped γ-Al_2O_3	0-3.36	1000	14	24	Y	29
Ga_2O_3/γ-Al_2O_3 La_2O_3/γ-Al_2O_3 La_2O_3/Ga_2O_3/γ-Al_2O_3	5-30/95-70 6/94 6-15/30/64-55	500	75	20	N	13
CeO_2-ZrO_2-γ-Al_2O_3	10:10:80	500	75	50	N	15
Aluminum borate	Al:B=10	750	100	48	Y	27
Mn/Al_2O_3 La-Mn/Al_2O_3 Fe-La-Mn/Al_2O_3	6%MnO, 3%La_2O_3, 4%Fe_2O_3	80-300	8	9	N	16
Aluminophosphate	Al:P=6	750	NA	48	N	14
ZSM-5 zeolite	Si/Al=27.1	1000-1175	100	10	Y	30
Alkali-ZSM-5 zeolite					Y	30
La-, Ce-, Pr-, Nd-doped Y zeolite	11.17-12.86	800	100	2-17	Y	31
H-ZSM-5	SiO_2/Al_2O_3 = 80	500	100	30	N	17
Cu-ZSM-5	Si/Al=25; 1.63-2.16 wt.%Cu	450-500	2-2.5	7	Y	18
Y-zeolite	SiO_2/Al_2O_3 > 150	1000-1200	50	4	N	32
Na-beta zeolite La-beta zeolite	SiO_2:Al_2O_3=10; 300 15 wt.% La loading	800	5	200	Y	33
Cu-beta zeolite	SiO_2:Al_2O_3= 38; 4.3 wt.%Cu	500-900	5	3	Y	19

Green Chemistry Accepted Manuscript

Ce-ZSM-5	Si/Al=17.1; 22.6; 146.6				Y	
Ce-beta zeolite	Si/Al=12	600	10-12	3-99	N	20
Ce-Y zeolite	Si/Al=2.8				N	
Beta zeolite	Pure zeolite	800	10	0.5	Y	21
MCM-41, MCM-48	100%SiO_2	600	100	2	N	34
Co-, Ni-doped SiO_2	0-100 wt.%Co or Ni	500	100	0-60	N	35, 36
Ni/SBA-15	10 wt.%Ni	500, 650	90	20	Y	10
Nb-SBA-15	n_{Si}/n_{Nb}=5,10	100-600	100	12-168	N	11
MCM-41, MCM-48, HMS, SBA-15, KIT-1, FSM-16, PCH	Pure silica	400	30	48-120	Y	12
Ni/TiO_2, Ni/ZrO_2	10 wt.% Ni	500, 600	90	20 h	N	10

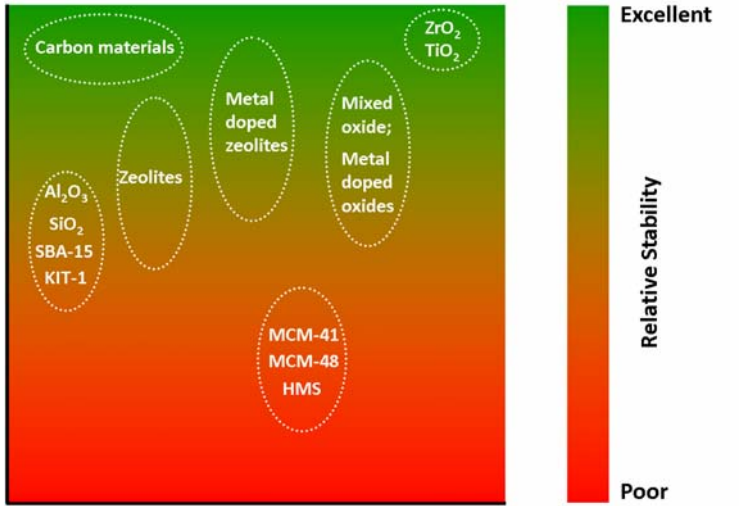

Fig. 3. Illustration of hydrothermal stability of heterogeneous catalysts in superheated steam (T > 400 °C).

2.2. Liquid water below 200 °C

Numerous biomass-related reactions are carried out in liquid water at temperatures below 200 °C, such as hydrolysis,[37] dehydration,[38] isomerization, oxidation as well as aldol condensation,[39] and hydrogenation. As seen in section 2.1, some oxides can withstand hydrothermal treatments in superheated steam when the temperature is not very high (usually less than 400 °C). However, when these same oxides are used in liquid water, the oxide structure may change drastically even at low temperatures, i.e. less than 200 °C.

Silica-based materials MCM-41 has been found to lose its ordered hexagonal mesoporous structure when subjected to boiling water for 12 h.[8] This structural loss involved silicate hydrolysis in the presence of water. Similar to the trend in superheated steam, SBA-15 was more stable than MCM-41 and the BET surface area decreased slightly from 780 to 690 m^2/g after heating in boiling water for 24 h.[40] In contrast, the ordered structure of MCM-41 was completely lost after heating it in boiling water for only 6 h. Pollock et al.[41] found that the hydrothermal stability of mesoporous silica was critical for the catalytic processing of biofuels. In their study, SBA-15 was treated in liquid water at temperatures from 115 to 155 °C for 3 h under autogenic pressure. The results are consistent with a degradation mechanism in which silica dissolves from regions of small positive curvature, e.g., near entrances into the secondary pore network, and was redeposited deeper into the framework (Fig. 4a and b). Pore volume decreased quickly for the micropores but more slowly for the larger secondary mesopores. When it was treated in water at

Green Chemistry Accepted Manuscript

115 °C, the primary mesopore diameter increased along with a significant decrease in the intrawall void fraction. At 155 °C, the entrances to the secondary pore network completely closed, trapping water in the pore structure (Fig. 4c).

Fig. 4. Schematic graphical representation of the dissolution of silica from regions of small positive radius of curvature at the intersection of the secondary pore network and the primary mesopores of radius r_1, and redeposition in micropores as well as the entrance to the secondary pore network in regions of small negative radius of curvature. In the process (top to bottom), the void fraction decreases and the mesopore diameter increases from r_i to r_f.[41] Reprinted with permission from Ref. 41 (Rachel A. Pollock, Gennady Yu. Gor, Brenna R. Walsh, Jason Fry, I. Tyrone Ghampson, Yuri B. Melnichenko, Helmut Kaiser, William J. DeSisto, M. Clayton Wheeler, and Brian G. Frederick, J. Phys. Chem. C 2012, 116, 22802-22814). Copyright (2014) American Chemical Society.

In contrast to pure silica, we find improved stability with organo-silica materials. For example, methylene-, ethylene-, and phenylene-bridged periodic mesoporous organosilicas (PMOs) exhibited significantly better hydrothermal stabilities than periodic mesoporous silica in boiling water for 18 h.[42] The high hydrothermal stability observed in the nanoporous PMOs materials may be due to their thicker pore walls (26-35 Å) after synthesis, compared to 24 Å for mesoporous silica. For the selective production of furfural (FUR) from xylose at 160-180 ^{o}C, an arenesulfonic modified mesoporous SBA-15 has been reported to have improved hydrothermal stability after reaction for 20 h.[43] Due to the stable arenesulfonic-sites and pore structures during reaction, the arenesulfonic SBA-15 catalysts achieved high FUR yield of 80% at 99% conversion for reactions at 160 °C. The catalyst aged at 160 ^{o}C was not deactivated after reactions at 160 ^{o}C while its surface acidity dropped after reactions at 180 ^{o}C due to enhanced cleavage of the aryl ring-silica bond via hydrolytic attack. On the other hand, the catalyst aged at 180 °C showed negligible acid-site leaching effects for the studied reaction temperatures.

Zeolites The hydrothermal stability of zeolites in aqueous solutions (acid or base) has been explored in previous studies. The results showed that Al was removed preferentially at low pH, while Si was dissolved primarily at high pH.[44] Previous work on the stability of zeolites and related materials (Al_2O_3 and SiO_2) in pure water at high temperatures (≥ 130 ^{o}C) concluded that the role of OH^--catalyzed Si dissolution and H^+-catalyzed Al dissolution also depends on the framework configuration, SiO_2/Al_2O_3 ratio (Si/Al ratio) and the type of cation. Increasing the Si/Al ratio of zeolites is an effective way to improve catalyst stability in aqueous environments because it increases the hydrophobic character of the zeolite.[45] For example, Al-free hydrophobic Sn-beta zeolites have been successfully used as weak Lewis acid sites to isomerize glucose to fructose in an acidic aqueous environment.[46]

When using different zeolites as catalysts in the dehydration of fructose to 5-hydroxymethyl furfural (HMF) under liquid water (130 ^{o}C), about 1-2 wt% of the zeolite has been found to dissolve in the solution.[44] This resulted in a solution of aluminosilicate species with Al 1.2-26.2 mg/L and Si up to 226 mg/L. The actual concentration of these species depends on the zeolite type used and on its Si/Al ratio. Several dissolved Al and Si salts were observed (e.g., aluminum formate, $Al(HCO_2)_3$, aluminumlactate, $Al(C_3H_5O_3)_3$, and $AlCl_3$). The active species dissolved from the zeolites are probably oligomeric aluminosilicate fragments in which the Al-O-Si and Si-

Green Chemistry Accepted Manuscript

O-Si connectivity is found to be similar to that of amorphous aluminosilicate solids that do not catalyze hexose isomerization reactions.

For the bio-oil upgrading in liquid water (200 ^{o}C and 47.6 atm), the stability of hydrophilic and hydrophobic HY zeolites has been compared.[45] It was found that the structure of the hydrophobic sample functionalized by octadecyltrichlorosilane remained largely undisrupted after exposure to the aqueous environment at 200 °C. By contrast, the crystalline structure of an untreated HY zeolite collapsed in a few hours in contact with a liquid medium at 200 °C.

Functionalized porous supports Functional groups, such as sulfonic acid, are generally used as acid catalysts in biomass conversion after grafting onto solid supports. The hydrothermal stability of five solid acid catalysts (Dowex50WX2, Amberlyst 15, Amberlyst 36, silica sulfuric acid and $Cs_{2.5}H_{0.5}PW_{12}O_{40}$ supported on K-10 clay ($Cs_{2.5}$/K-10, 30 wt.%)) has been studied during upgrading of a model bio-oil (phenol/water/acetic acid/acetaldehyde/hydroxyacetone/D-glucose/2-hydroxymethylfuran) at 120 ^{o}C for 3 h.[39] The upgrading involved many simultaneous competing reactions including esterification, etherification, olefin hydration, phenol alkylation, aldol condensation, sugar dehydration etc. It was revealed that SiO_2-SO_3H exhibited the highest water tolerance under these conditions. However, deactivation of a sulfonic acid (-SO_3H) functionalized mesoporous silica (MCM-41) occurred rapidly after only one reaction cycle during catalytic conversion of cellulose into alkanediols at 150-230 ^{o}C because of an irreversible change in the mesoporous structure and loss of acid groups.[47] Likewise, in the selective production of furfural during xylose cyclodehydration in the liquid phase at 140 ^{o}C for 20 h, water was found to enhance the cleavage of silica-propylsulfonic bonds in the functionalized SBA-15, resulting in loss of the acid sites.[48]

However, propylsulfonic acid functionalized ordered silicas are more stable than propylsulfonic acid modified amorphous silica. For example, for the production of 5-hydroxymethylfurfural (HMF) from fructose in a solution of THF and H_2O (4:1 w/w) at 13.6 atm and 130 ^{o}C, a propylsulfonic acid-modified amorphous silica was the least stable compared to three propylsulfonic acid-functionalized ordered silicas (one inorganic SBA-15-type silica, and two ethane-bridged SBA-15-type organosilicas).[49] Furthermore, similar to the hydrothermal stability trend in superheated steam, the organosilicas are more stable and maintained a steady catalytic activity longer than the inorganic SBA-15-type silica. The deactivation under flow conditions is caused primarily by hydrolytic cleavage of acid sites. The positive effect of the presence of the ethane groups on the hydrothermal stability of acid functionalized mesoporous organosilicas was also seen in another study of sulfonic acid functionalized mesoporous organosilicas synthesized by one-step condensation (ethane groups bridged in the framework).[50] The results showed that the presence of hydrophobic ethane groups in the framework positively affected the hydrothermal stability and catalytic activity in the esterification of ethanol with acetic acid, and that even a small fraction of bridging ethane groups (25 mol%) in the framework could lead to mesoporous organosilicas with improved hydrothermal stability (in boiling water for 48 h).

Besides grafting on oxides, sulfonic acid has been immobilized on carbon materials and used as catalyst in biomass conversion. In the hydrolysis of cellulose to glucose under hydrothermal reactions at temperatures of ca. 150 ^{o}C,[37, 51, 52] the sulfated, sulfonated activated-carbon catalysts showed remarkably high yield of glucose, which was due to the high hydrothermal stability and the strong acid sites of SO_3H functional groups.[52] In the selective decomposition of the hexose sugars, glucose and fructose to levulinic acid (LA) at 200 ^{o}C, the sulfonated graphene oxide catalysts (GO-SO_3H) showed good stability and high LA yield.[53]

Other materials It is well known that 5-hydroxymethylfurfural (HMF) is a versatile intermediate for the production of biofuels and value-added chemicals and it can be produced by dehydration of glucose/fructose in liquid water. In this respect, niobic acid ($Nb_2O_5{\cdot}nH_2O$) has been studied as a Lewis acid catalyst for the dehydration of glucose to HMF in aqueous phase at 130-170 ^{o}C.[38, 54] The niobic acid showed high stability. Likewise, novel CoAl-hydrotalcite catalysts with different Co^{2+}/Al^{3+} ratios have also been employed for the selective dehydration of

Green Chemistry Accepted Manuscript

D-fructose into HMF.[55] The spent CoAl-hydrotalcite catalysts were easily recycled and showed high catalytic stability over three consecutive runs. In the hydrolysis of cellulose to glucose over a heteropoly acid $H_3PW_{12}O_{40}$ (80 ^oC, 2 h), a high yield of glucose (50.5%) and selectivity higher than 90% was achieved due to its high hydrothermal stability.[56]

Recently, model compounds containing sulfonic acid groups linked to aromatic, alkane, or cycloalkane carbon atoms have been investigated under hydrothermal conditions (100-160 ^oC for 24 h in water).[57] The aromatic-sulfonic acid compounds degraded readily, while the hydrolysis of the alkyl sulfonic acid linkages was negligible. Therefore, hydrothermally stable sulfonic-acid catalysts need sulfonic acid attached via alkyl linkers.

The hydrothermal conditions and stability of heterogeneous catalysts in liquid water at T < 200 ^oC is summarized in Table 2.

Table 2 Hydrothermal stability of heterogeneous catalysts in liquid water at T < 200 ^oC

Catalyst	Liquid water (T < 200 ^oC)			Structure change (Y/N)	Ref.
	Temperature (^oC)	Pressure	Time (h)		
MCM-41	Boiling water	1 atm	6, 12	Y	8, 40
SBA-15	Boiling water	1 atm	24	N	40
SBA-15	115-155	autogenic	3	Y	41
Methylene-, ethylene- and phenylene-bridged periodic mesoporous organosilicas	Boiling water	1 atm	18	N	42
Arenesulfonic modified SBA-15	160, 180	autogenic	20	N	43
MCM-41-SO_3H	150-230	autogenic	NA	Y	47
Propylsulfonic-SBA-15	140	autogenic	20	Y	48
SBA-15	130	13.6 atm	NA	Y	49
Ethane-bridged SBA-15 organosilicas	130	13.6 atm	NA	N	49
Zeolite	130	autogenic	NA	Y	44
HY zeolite	200	47.6 atm	NA	Y	45
Octadecyltrichlorosilane functionalized HY zeolite	200	47.6 atm	NA	N	45
Sulfonic acid functionalized mesoporous organosilicas	Boiling water	1 atm	48	N	50
Sulfonated activated-carbon	150	autogenic	NA	N	37, 51
Nb_2O_5•nH_2O	130-170	autogenic	NA	N	38, 54
Nb_2O_5•nH_2O	200	autogenic	NA	Y	38
$H_3PW_{12}O_{40}$	180	autogenic	2	N	56
ZrO_2/CNT	95	autogenic	6	N	58

2.3. Liquid water at elevated temperatures (≥ 200 ^oC)

Liquid water at elevated temperatures (≥ 200 ^oC) is much more corrosive than liquid water at temperatures below 200 ^oC discussed previously. This is reflected in the fact that many mesoporous oxide materials maintain their structure in boiling water at atmospheric pressure, while their pore structures completely collapse in the aqueous-phase conditions at elevated

Green Chemistry Accepted Manuscript

temperatures (≥ 200 °C). [29, 40, 46, 59,] Similar differences in the stability of other heterogeneous catalysts are seen when subjected to aqueous-phase conditions at elevated temperatures (≥ 200 °C).

Silica- and alumina-based materials When pretreating in liquid water at 200 °C for 12 h, SBA-15 loses 96% of its surface area as a result of a complete collapse of the ordered mesopores, leading to loss of its structural integrity.[59] Likewise, at 200 °C and autogenic pressure, the structures of γ-Al_2O_3, Ni/γ-Al_2O_3, and Pt/γ-Al_2O_3 catalysts changed due to the transformation of the γ-alumina phase into a hydrated boehmite (AlOOH) phase, with a significantly decreased acidity and surface area.[60] For metal-free γ-alumina, the transformation is completed within 10 h, whereas the presence of nickel or platinum particles significantly retards the formation of boehmite. In the early stages of this treatment the surface area of γ-alumina increases, suggesting surface pitting and formation of small boehmite particles on the surface of γ-alumina. This process is followed by the formation of a compact crystalline boehmite phase. It was proposed that the metal particles affected the kinetics of this transformation by blocking specific surface hydroxyl groups that act as initial hydration sites. Furthermore, the transformation of γ-alumina into boehmite was accompanied by sintering of the supported metal particles.

In aqueous-phase reforming of ethylene glycol and glycerol, γ-Al_2O_3 supported Pt catalysts were unstable as expected and underwent phase transformation to boehmite [AlO(OH)].[61, 62] The transformation into boehmite proceeded at even milder conditions (210 °C, 39.5 atm).[63] Koichumanova et al. found that Pt/γ-Al_2O_3 deactivated irreversibly in aqueous phase because the Pt surface area decreased owing to an increasing metal particle size and coverage of the active surface with boehmite.[63] Due to this phase transformation of alumina, it was demonstrated that the use of boehmite instead of gamma alumina might lead to improved stability.[63] Indeed, the rate of formation of hydrogen per Pt surface atom is significantly higher on boehmite compared to the alumina-supported catalyst. Lehnert et al. also found that variation of support materials from pure γ-alumina to a mixture of γ-, δ- and θ-phases led to an increase in hydrogen production from 1.2×10^{-3} to 7.6×10^{-3} mol min^{-1} g_{cat}^{-1}.[62]

On the other hand, the presence of carbohydrates in aqueous phase conditions can form dissolution-inhibiting carbonaceous deposits on the oxide surface and improve the material stability.[59, 64] Such effects were demonstrated for a 1 wt.% Pt/γ-Al_2O_3 catalyst used in the depolymerization of various kinds of lignin in an ethanol/water mixture at 225 °C and autogenic pressure.[64] In the absence of reactants, the γ-alumina support was found to transform into boehmite within 4 h, leading to a reduction in support surface area, sintering of the supported Pt nanoparticles, and a reduction of active metal surface area. Addition of aromatic oxygenates to mimic the compounds typically obtained by lignin depolymerization leads to a slower transformation of the support oxide (Fig. 5a). These compounds, however, were not able to slow down the decrease in dispersion of the Pt nanoparticles (Fig. 5b). It was found that vanillin and guaiacol (a lignin-derived model compound) stabilize the aluminum oxide more than phenol, anisole, and benzaldehyde because of the larger number of oxygen functionalities that can interact with the alumina (Fig. 5b). The catalyst treated in the presence of lignin showed almost no formation of boehmite, no reduction in support or active metal surface area, and no Pt nanoparticle sintering (Fig. 5b and c). Furthermore, in the absence of lignin-derived aromatic oxygenates, ethanol forms a coke-like layer on the catalyst, while oxygenates prevent this by adsorption on the support by coordination via the oxygen functionalities. In contrast, in the transetherification of guaiacol to *o*-ethoxyphenol in supercritical ethanol in the presence of water produced (280 °C for 3 h with autogenic pressure),[65] the authors found that water deactivated γ-Al_2O_3 by competitive adsorption with guaiacol on the surface and water also caused the loss of the specific surface area of γ-Al_2O_3 due to the formation of the boehmite phase. The difference in behavior is likely due to the reaction temperature being much higher.

Green Chemistry Accepted Manuscript

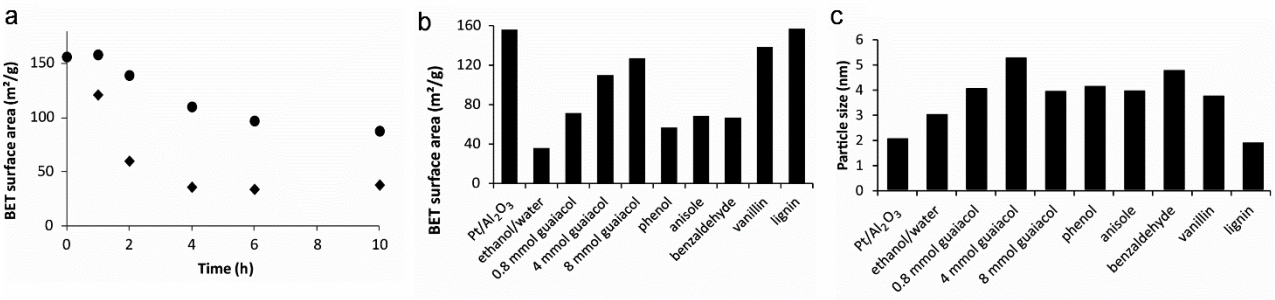

Fig. 5. BET surface area (a and b) of a 1 wt % Pt/Al_2O_3 catalyst after treatment with and without guaiacol at 225 °C: (♦) Samples treated in ethanol/water and (●) samples treated in ethanol/water with 4 mmol of guaiacol, and (c) average diameter of Pt nanoparticles of an untreated 1 wt % Pt/Al_2O_3 catalyst and of a 1 wt % Pt/Al_2O_3 catalyst after 4 h treatment at 225 °C in various aromatic oxygenate solutions. Modified from Ref. [64]. Reprinted with permission from Ref. 63 (Anna L. Jongerius, John R. Copeland, Guo Shiou Foo, Jan P. Hofmann, Pieter C. A. Bruijnincx, Carsten Sievers, and Bert M. Weckhuysen, ACS Catal. 2013, 3, 464-473). Copyright (2014) American Chemical Society.

Zeolites In section 2.2, we have shown that zeolites have relatively poor hydrothermal stability in liquid water at T < 200 °C. Thus, there are few studies on the stability of zeolites in liquid water at T ≥ 200 °C. Ravenelle and coworkers [66] systematically investigated the hydrothermal stability of zeolites Y and ZSM-5 with varying Si/Al ratios in liquid water at 150 °C and 200 °C under autogenic pressure. They found that during treatment in hot water, zeolite Y with a Si/Al ratio of 14 or higher transformed into an amorphous material, and the rate of this degradation increased with increasing Si/Al ratio. In contrast, ZSM-5 was not modified under the same conditions. The main degradation mechanism was suggested to be hydrolysis of the siloxane bonds (Si-O-Si) as opposed to dealumination, which dominates under steaming conditions. In the resulting amorphous phase, Al remains tetrahedrally coordinated, but the micropore volume and concentration of accessible acid sites is reduced dramatically.

Mixed oxide materials Mixed oxides have better stability than corresponding pure oxides under superheated steam. Similar improvement is seen for mixed oxides in liquid water at T ≥ 200 °C. In the hydrolysis of cellobiose into glucose under liquid water at 200 °C, amorphous silica-alumina (ASA) is much more hydrothermally stable than pure silica or alumina.[67] The synthetic procedure used plays a major role in its resultant stability: ASA prepared by cogelation (CG) lost its microporous structure owing to hydrolysis of the siloxane bonds, but the resulting mesoporous material still had a considerable surface area. ASA prepared by deposition precipitation (DP) contained a silicon-rich core and an aluminum-rich shell. In hot liquid water, the latter structure was transformed into a layer of amorphous boehmite, which protected the particle from further hydrolysis. The surface area showed relatively minor changes during the transformation. The superior stability of SiO_2-Al_2O_3 was also reported in the conversion of sorbitol to alkanes over a Pt/SiO_2-Al_2O_3 catalyst at 225 °C and autogenic pressure (held for 2 h) in aqueous medium.[68] The authors found that catalyst was less sensitive in liquid water after a pre-treatment by steaming, in terms of platinum dispersion and textural properties.

Over silica-alumina, BET surface area of niobium phosphate ($NbOPO_4$), and niobic acid ($Nb_2O_5 \cdot nH_2O$) decreased upon treatment with liquid water at 240 °C for 3 h for butanol dehydration.[69] The surface area of amorphous niobic acid decreased significantly from 118 to 17 $m^2\ g^{-1}$. This decrease was a result of its poor hydrothermal stability under high pressure and temperature through pore degradation and phase transformation from high surface area metastable phases to low surface area phases.

In our previous work we have investigated the hydrothermal stability of amorphous niobia and niobia-silica composites in aqueous phase dehydration of 2-butanol.[70] Although loss of surface area occurred for all of the niobia and niobia-silica catalysts, the surface area loss

Green Chemistry Accepted Manuscript

occurred to lesser extent for the Nb-Si oxide catalysts. The addition of only a small amount of SiO_2 (5 wt%) was found to improve the stability of niobia-silica composites. In these samples, the regions that contained more silica retained their porous structure after reaction while those areas with depleted silica content transformed into crystalline niobia. It was concluded that addition of silica to niobia improves the stability of the support by preventing crystallization. The hydrothermal stability of Nb_2O_5/SBA-15 composite prepared by atomic layer deposition (ALD) has been also investigated in our recent work.[71] Mesoporous materials after ALD deposition of niobia maintained the structural organization of SBA-15. Materials where 10, 19, and 30 ALD cycles of niobia were deposited showed remarkable hydrothermal stability, with minimal change in porosity and structural properties upon treatment in liquid water at 200 ^{o}C. The mesoporous niobia/SBA-15 material produced by 19 cycles was studied as an acid catalyst for the aqueous-phase dehydration of 2-butanol, showing catalytic activity superior to commercial niobia.

For the aqueous-phase hydrodeoxygenation of sorbitol under 245 ^{o}C and 61.3 atm, the Pt/Zr-P catalyst undergoes phase transformations of amorphous into crystalline Zr-P having a rhombohedral framework along with a 97% loss of surface area, 86% loss of Pt surface sites and 95% loss of surface acid sites during the reaction.[72] However, a Pt-ReO_x/C catalyst has a higher hydrothermal stability than Pt/Zr-P and only lost 17% of its surface area during the reaction. This indicated that zirconium phosphate is not a stable support, while the activated carbon (Norit Darco) is hydrothermally stable.

Carbon materials and oxide/carbon composites Ordered mesoporous carbon (OMC) supported platinum catalysts have been used in aqueous-phase reforming (APR) of ethylene glycol (EG) for hydrogen production.[73, 74] Characterization results revealed that an ordered mesostructure, high surface area, large pore volume, and uniform mesopore size was maintained along with a high dispersion of platinum nanoparticles after APR of EG at 250 °C and 45 atm over 24 h. These results showed that the structure of the ordered mesoporous carbon support exhibited outstanding hydrothermal stability in APR under high pressure and temperature.

A ZrO_2/CNT composite was recently synthesized by a grafting method followed by high-temperature annealing.[58] The oxygen-containing functionalities on CNT surface uniformly disperse and stabilize the ZrO_2 nanoparticles under hydrothermal conditions. This ZrO_2/MWCNT withstands decomposition and no ZrO_2 leaching was found under aqueous phase at both 95 ^{o}C and 220 ^{o}C, providing potential applications in the catalysis of biomass conversion under aqueous phase conditions.

We investigated the hydrothermal stability of niobia/carbon composites in liquid water at elevated temperatures (≥ 200 ^{o}C). We found that the niobia/carbon composites prepared by a deposition precipitation-carbonization (DPC) method were hydrothermally stable in butanol aqueous-phase dehydration.[75] The catalysts generated by the DPC method contained highly dispersed niobia nanoparticles (ca. 8 nm) embedded in carbon, which helps to prevent the growth of oxide crystallite size. We also compared the hydrothermal stability of niobia supported on carbons (carbon black and carbon nanotubes) prepared by impregnation and deposition precipitation (DP) in the aqueous phase.[76] At 14.8 atm and 200 °C, large niobia particles were formed due to crystallization of niobia/carbon composites prepared by impregnation. In contrast, no large particles were formed on niobia/carbon composites prepared by DP. For the aqueous phase dehydration of 2-butanol at 51.3 atm and 240 °C, deactivation was observed on the niobia/carbon catalyst prepared by impregnation due to the formation of large niobia particles. The niobia/carbon catalyst prepared by DP exhibited high catalytic activity, which was stable for over 40 h.

Table 3 Hydrothermal stability of heterogeneous catalysts in liquid water at T ≥ 200 ^{o}C

Catalyst	Superheated steam			Structure change (Yes/No)	Ref.
	Temperature (^{o}C)	Pressure	Time (h)		

Green Chemistry Accepted Manuscript

SBA-15	200	autogenic	12	Y	59, 71
SiO_2	200	autogenic	12	Y	59
γ-Al_2O_3, Ni/γ-Al_2O_3, and Pt/γ-Al_2O_3	200	autogenic	10	Y	60
Pt/γ-Al_2O_3	220	24.7 atm	37	Y	61
Pt/γ-Al_2O_3	250	19.7 atm	10	Y	62
Pt/γ-Al_2O_3	210, 270	39.5, 88.8 atm	NA	Y	63
Pt/γ-Al_2O_3	225	autogenic	4	Y	64
Y-Zeolite (Si/Al=14)	200	autogenic	6	Y	66
ZSM-5	200	autogenic	6	N	66
Pt/Al_2O_3-SiO_2	225	autogenic	2	N	68
Nb_2O_5-SiO_2	200	autogenic	12	N	70
Pd/Nb_2O_5	200	autogenic	12	Y	70
Pt on mesoporous carbon	250	44.4 atm	24	N	73, 74
Nb_2O_5/Carbon	240	51.3 atm	100	N	75
ZrO_2/CNT	220	autogenic	6	N	58

The hydrothermal conditions and stability of heterogeneous catalysts in liquid water at T ≥ 200 °C are summarized in Table 3. An illustration is provided to present a graphical overview of the relative stability of these materials in liquid water at temperatures below the critical point of 373.9 °C (Fig. 6).

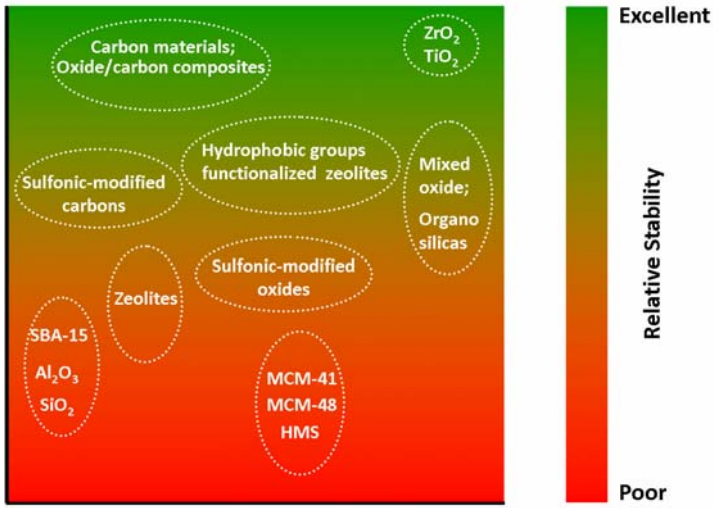

Fig. 6. Illustration of hydrothermal stability of heterogeneous catalysts and catalyst supports in sub-critical liquid water (T < 374 °C).

2.4. Supercritical water conditions

It is well known that supercritical water (SCW) above the thermodynamic critical point (T_c=373.95 °C, P_c=217.75 atm) behaves very differently from liquid water. As water is heated along its vapor-liquid saturation curve, its dielectric constant decreases due to the hydrogen bonds between water molecules being fewer and less persistent. The reduced dielectric constant enables hot compressed water to solvate small organic molecules, allowing organic reactions to occur in a

Green Chemistry Accepted Manuscript

single fluid phase (supercritical water).[5] Therefore, the development of stable catalytic support materials for reactions carried out in SCW is of great importance. So far, γ-alumina and carbon materials have been used as catalyst supports for biomass-related reactions (mainly reforming and gasification) in supercritical water.

The catalytic reforming of ethylene glycol (5 and 15 wt%) has been studied on alumina-supported mono- and bi-metallic Ir, Pt and Pt-Ni catalysts in supercritical water up to 450 °C and 246.7 atm.[77, 78] All fresh catalysts had surface areas of ~200 m^2/g and the surface areas decreased to ~20 m^2/g during the reaction. This decrease was found to happen during the initial stage of the reaction (within the first 15 min) and also occurred when only water (without organic reactants) was used. The decreasing surface area was attributed to phase change of the γ-Al_2O_3 to boehmite as expected. The existence of small amount of α-Al_2O_3 was also noticed after the reaction. The phase change to boehmite occurred during start-up of the reaction and the catalyst was stable after this initial period.[78] A Pt-Ni/Al_2O_3 with a total metal loading of 1.5 wt% (molar ratio Pt:Ni = 1) was identified as a promising catalyst for the reforming of ethylene glycol in supercritical water. The high dehydrogenation activity of Pt-Ni catalysts suppressed the formation of acetic acid. Acetic acid was found to be responsible for hydroxylation of the Al_2O_3 support, leading to migration and coverage of the metal particles by $Al(OH)_x$ and resulting in deactivation of the Pt-based catalysts. However, it was reported earlier by Wawrzetz et al. that the phase change from γ-Al_2O_3 to boehmite did not cause blocking or deactivation of the catalytic sites.[79]

In SCW, the extent of transformation of γ-Al_2O_3 to corundum increases with increasing temperature, due to the expected transformations of alumina (γ→δ→θ→α). The surface area decreases with each step and the final transition to the alpha phase is associated with the greatest drop in surface area. Elliott et al.[80] have reported that after the exposure of different forms of alumina in sub- or supercritical water (350 ^oC and 197.4 atm), δ- and γ-Al_2O_3 were completely hydrolyzed to give boehmite, while η-Al_2O_3 formed a mix of boehmite and α-Al_2O_3 leading to loss of surface area. De Vlieger and coworkers' results have also presented similar observations of phase change and instability of γ-Al_2O_3 in a continuous flow reactor for the reforming of ethylene glycol in supercritical water.[78] However, their study on catalyst screening for the hydrothermal gasification of bio-oil indicated that such phase changes of γ-Al_2O_3 were not seen in supercritical water (500 ^oC and 276.3 atm).[81] They ascribed this to the experimental conditions used, such as type of reactor and a short reaction time (15 min). The changes in BET surface area for different supports is shown in Fig. 7.[81] A slight increase in the surface area of the catalyst is noticed with ZrO_2, TiO_2 and Ce-ZrO_2 after the reaction and this additional gain in the surface area can be associated with the deposition of internal coke in the catalyst. This indicated that titania, zirconia and modified zirconia (Ce-ZrO_2) are stable supports for hydrothermal gasification of biomass. They observed a slight surface area loss for Al_2O_3 and a significant loss in the surface area of silica and activated carbon, indicating that silica and activated carbon used are unsuitable supports for hydrothermal gasification of biomass in SCW. Because carbon materials are generally hydrothermally stable, we infer that the decrease of surface area of the activated carbon is due to the gasification of activated carbon at 500 ^oC.

Green Chemistry Accepted Manuscript

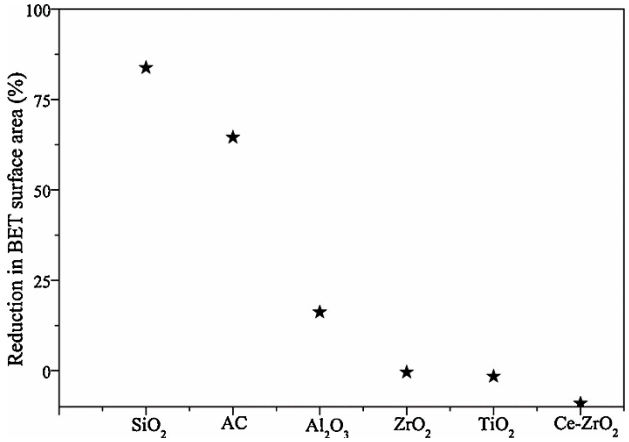

Fig. 7. Percentage reduction of catalyst surface area loss after 15 min of reaction time (The percentage reduction of the BET surface area is defined as the ratio of final surface area after the reaction to the initial surface area).[81] Reprinted from Catalysis Today, 195, Anand G. Chakinala, Jithendra K. Chinthaginjala, Kulathuiyer Seshan, Wim P.M. van Swaaij, Sascha R.A. Kersten, Derk W.F. Brilman, Catalyst screening for the hydrothermal gasification of aqueous phase of bio-oil, 83-92, Copyright (2014), with permission from Elsevier.

Recently, several carbon materials have been recognized as hydrothermally stable supports for catalytic conversion of biomass-related chemicals in SCW.[76, 82, 83] For example, carbon nanotubes (CNTs) are believed to be attractive supports due to their significant physical and chemical properties (stability, high heat conductivity and open structure) and have already been explored to produce renewable chemicals from biomass in supercritical water (SCW).[83] The result showed that CNTs represent the most promising hydrothermally stable catalyst support for the production of hydrogen by reforming of ethylene glycol and acetic acid in SCW (450 ^{o}C and 246.7 atm).

Hydrothermal conditions and stability of heterogeneous catalyst in supercritical water are summarized in Table 4. In conclusion, carbon-, TiO_2- and ZrO_2-based materials are stable supports in supercritical water, while Al_2O_3- and SiO_2-based materials are not stable, as expected based on their performance at lower temperatures.

Table 4 Hydrothermal stability of heterogeneous catalysts in supercritical water

Catalyst	Supercritical water			Structure change (Yes/No)	Ref.
	Temperature (^{o}C)	Pressure (atm)	Time (h)		
Mono-, bi-metallic Ir, Pt and Pt-Ni on γ-Al_2O_3	450	246.7	0.25	Y	77, 78
γ-Al_2O_3	350	197.4	NA	Y	80
TiO_2, ZrO_2 and Ce-ZrO_2	500	276.3	0.25	N	81
Al_2O_3, SiO_2 and activated carbon	500	276.3	0.25	Y	81
Pt/CNT	450	246.7	6	N	83

NA=not available

2.5. Mechanism of structure changes under hydrothermal conditions

The review of the literature shows that the morphology and structure of metal oxide supports changes dramatically under hydrothermal conditions. For example, silica- and alumina-based materials are subject to hydrolysis of Si-O-Si or Al-O-Al bonds, which causes dissolution, leading to the collapse of pores and loss of surface area. In contrast, carbon materials are

Green Chemistry Accepted Manuscript

hydrothermally stable due to covalent carbon-carbon bonds which are more difficult to hydrolyze. The mechanism of degradation and the stability of oxide supports is markedly affected by the nature and severity of the hydrothermal conditions used. For example, in superheated steam, the structural change of zeolites is predominantly due to the hydrolysis of Si-O-Al bonds, leading to dealumination. Whereas in liquid water at temperatures > 100 ^{o}C, the main degradation mechanism of zeolites is thought to be the hydrolysis of the siloxane bonds (Si-O-Si). Furthermore, in liquid water, the mechanism of structural changes in zeolites and mesoporous silica-alumina can be significantly affected by the pH of the solution as shown in Scheme 1.[66] The Si-O-Al hydrolysis is catalyzed by the protons, whereas siloxane bond cleavage is catalyzed by hydroxyl ions. During the siloxane hydrolysis, a Si-O-Si bond is broken, and two silanol groups are formed. The base-catalyzed hydrolysis also occurs at Si-O-Al bonds, but they are more resistant to attack from water. In addition, Al in tetrahedral positions creates a net negative charge in the framework, which repels OH^- ions that are responsible for siloxane hydrolysis.

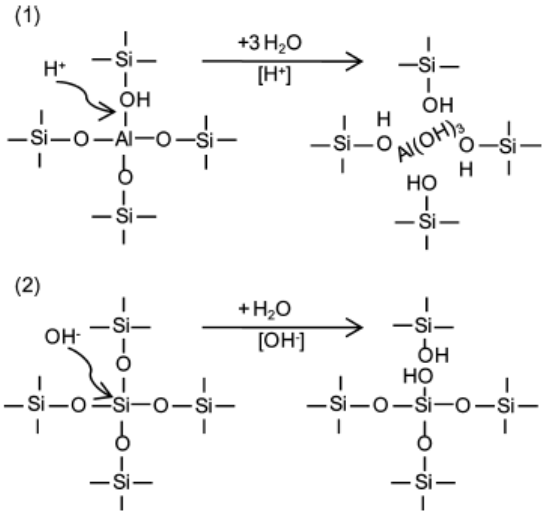

Scheme 1. Mechanisms for acid-catalyzed dealumination (1) and base-catalyzed hydrolysis of siloxane bonds (2).[66] Reprinted with permission from Ref. 65 (Ryan M. Ravenelle, Florian Schüβler, Andrew D'Amico, Nadiya Danilina, Jeroen A. van Bokhoven, Johannes A. Lercher, Christopher W. Jones, and Carsten Sievers, J. Phys. Chem. C 2010, 114, 19582-19595). Copyright (2014) American Chemical Society.

The mechanisms of dealumination of the ZSM-5 zeolite and the improvement of the stability of the La-modified ZSM-5 zeolite in superheated steam have been investigated using density functional theory (DFT).[84] It was demonstrated that because of the hydrogen bond interaction between the first adsorbed water molecule and the ZSM-5 zeolite framework, the Al-O bond is weakened and elongated. As the second water molecule is adsorbed, the Al-O bond near the second water molecule is further weakened and eventually broken because of the hydrogen bond interaction between the second adsorbed water molecule and the ZSM-5 zeolite framework. As more water molecules are adsorbed, the other Al-O bonds are broken sequentially resulting in a dealumination of the ZSM-5 zeolite. The introduced lanthanum coordinates with four zeolite framework oxygen atoms, strengthens the zeolite framework, being located above the framework Al atom, it increases steric hindrances and partially prevents polar water molecules from attacking the Al-O bond. These actions retard the weakening of the Al-O bonds and improve the hydrothermal stability of the ZSM-5 zeolite.

The hydrothermal stability of the support may also influence the metal phase. For example, the Pt particle size on a Pt/γ-Al_2O_3 catalyst increased due to the transformation of γ-Al_2O_3 to boehmite when subjected to hot water at T $\geq$ 225 ^{o}C.[63, 64] However, when hydrothermally stable

Green Chemistry Accepted Manuscript

carbon nanotubes (CNTs) were used as support at 450 ^{o}C and 247 atm, the metal Pt particles on Pt/CNT did not sinter, and no Pt leaching and/or phase change was found.[83]

3. Strategies for improving the hydrothermal stability of heterogeneous catalysts

3.1. Doping of the support by heteroatoms

According to the discussion in section 2, most oxides exhibit poor hydrothermal stability, especially in liquid water at elevated temperatures. The introduction of heteroatoms (such as La^{3+}, Ga^{3+}, Sm, Ce and Ti^{4+}) into these oxides has been reported to significantly improve their hydrothermal stability.[13, 17, 18, 66, 70, 85] Zahir and coworkers compared the hydrothermal stability of mesoporous γ-Al_2O_3 membrane with single and double dopant membranes.[13] Improvements in the hydrothermal stability of mesoporous γ-Al_2O_3 by transitional (Ga^{3+}) or rare-earth (La^{3+}) cations was observed, along with the enhanced effectiveness of double dopants (Ga^{3+}-La^{3+}).

The incorporation of Al^{3+} markedly improved the hydrothermal stability of the aluminosilicate MCM-41 materials compared to their pure silica analogues in boiling water.[86] The improvement in hydrothermal stability was found to be dependent on the Al content. Small amounts of Al (Si/Al=40.1) afforded much better protection of the mesoporous structure than larger amounts (Si/Al=8.5). A material with an intermediate amount of Al (Si/Al =23.1) exhibited intermediate stability. The influence of Al content on the hydrothermal stability is explained with respect to the position occupied by the framework Al within the MCM-41 pore wall, and it is suggested that Al incorporated on the surface/near surface region of the pore walls provided the greatest protection.

Our study showed that small amounts of silica (5 wt%) helped to improve the activity and hydrothermal stability of amorphous niobia in aqueous phase (200 ^{o}C for 12 h).[70] Although loss of surface area occurred for both pure niobia and niobia/silica composites after aqueous phase reforming, the surface area loss occurred to lesser extents for the Nb-Si oxide.

3.2. Surface modification

Surface modification can change the properties of the support by introducing new functionalities or removing hydrothermally unstable surface groups. Wei and coworkers [87] prepared amino-functionalized mesoporous silica SBA-16 by silylating N-(2-aminoethyl)-3-aminopropyltrimethoxysilane (AEAPS) on the SBA-16 supports. The functionalized SBA-16 samples showed superior hydrophobicity to the SBA-16 support, due to the replacement of silanol groups by amino-groups. The functionalized SBA-16 samples showed higher hydrothermal stability, which is related to the extent of silylation.

The hydrothermal stability of zeolites in hot liquid water can be improved by surface functionalization of octadecyltrichlorosilane (OTS).[45] This surface functionalization increased the hydrophobicity of zeolites without significantly reducing the density of acid sites. The hydrophobization with organosilanes makes the zeolites able to stabilize water/oil emulsions and catalyze reactions of importance in biofuel upgrading, i.e., alcohol dehydration and alkylation of m-cresol and 2-propanol in the liquid phase at high temperatures. Anchoring hydrophobic functionalities on the external surface causes the direct contact of bulk liquid water and the zeolite to be hindered, thus preventing the collapse of the framework during the reaction in liquid water. Furthermore, a clear difference was observed between hydrophobic and hydrophilic zeolites on the time evolution of conversion for the two zeolites (Fig. 8). The OTS functionalized zeolite shows a continuous increase in the m-cresol conversion with reaction time while the untreated zeolite loses its activity quite rapidly. For instance, the conversion on the hydrophobic zeolite from 3 to 5 h of reaction goes from 21 to 37%, while no change in conversion is observed with the untreated zeolite after 3 h, indicating that the hydrophilic catalyst is completely deactivated at this point.

Green Chemistry Accepted Manuscript

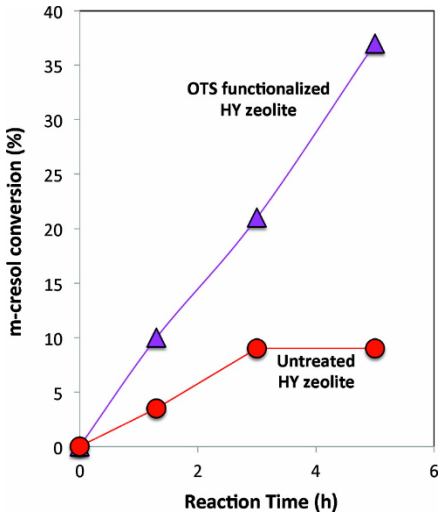

Fig. 8. Conversion of *m*-cresol as a function of reaction time during alkylation with 2-propanol at 200 °C and 47.6 atm in He over two HY zeolites (untreated and OTS-functionalized).[45] Reprinted with permission from Ref. 45 (Paula A. Zapata, Jimmy Faria, M. Pilar Ruiz, Rolf E. Jentoft, and Daniel E. Resasco, *J. Am. Chem. Soc.*, **2012**, *134* (20), 8570-8578). Copyright (2014) American Chemical Society.

3.3. Thin film coatings on the support

Mesoporous silica (SBA-15) has poor hydrothermal stability in liquid water at elevated temperatures (≥ 200 °C). This is because the hydrolysis of Si-O-Si bonds takes place when treated in hot water. Coating the hydrothermally unstable Si-O-Si surface by a thin-film can effectively inhibit the hydrolysis of the Si-O-Si and improve the hydrothermal stability. We used atomic layer deposition (ALD) to prepare thin-film niobia within the pores of SBA-15, as schematically shown in Fig. 9a.[71] Mesoporous materials after ALD cycles of niobia maintained the structural organization of SBA-15. The niobia coated silica showed remarkably improved hydrothermal stability, with minimal change in porosity and structural properties, upon treatment in liquid water at 200 °C. In the conversion of the γ-valerolactone to pentanoic acid, Pd catalyst supported on SBA-15-ALD-19 with 19 deposition cycles showed a substantially slower deactivation over the entire time-on-stream (Fig. 9b).

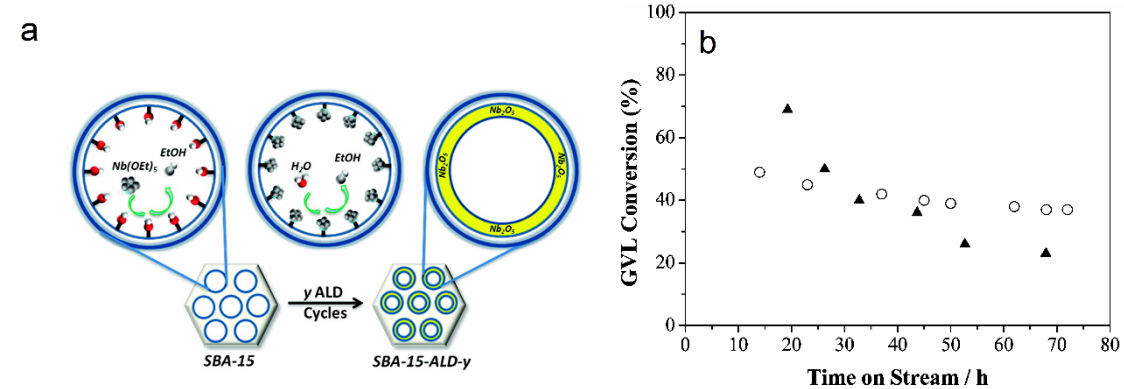

Fig. 9. (a) Illustration for the preparation of thin-film of Nb_2O_5 within the SBA-15 pore and (b) γ-valerolactone (GVL) conversion as a function of time-on-stream for (▲) Pd/HY-340 at 300 °C and 35 atm, WHSV 3 h^{-1} and (⚬) Pd/SBA-15-ALD-19 at 300 °C and 35 atm, WHSV 17 h^{-1}.[71] Reprinted with permission from Ref. 70 (Yomaira J. Pagán-Torres, Jean Marcel R. Gallo, Dong Wang, Hien N. Pham, Joseph A. Libera, Christopher L. Marshall, Jeffrey W. Elam, Abhaya K. Datye, and James A. Dumesic, *ACS Catal.*, **2011**, *1* (10), 1234–1245). Copyright (2014) American Chemical Society.

Green Chemistry Accepted Manuscript

However, the ALD process requires sequential reactions with two separate reactants and multiple cycles to achieve the thin-film coatings. Recently, we developed a simple and inexpensive approach to coat thin films of carbon onto metal oxide surfaces (SBA-15, amorphous silica and γ-alumina).[59] These carbon films provided improved hydrothermal stability for these oxides, which are not otherwise stable at elevated temperatures in the presence of liquid water. The structure of the carbon films is shown in Fig. 10.

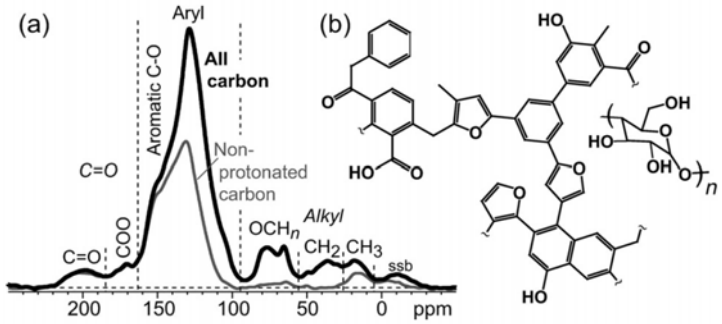

Fig. 10. a) Quantitative ^{13}C NMR spectra of all carbon atoms (thick line), and of nonprotonated carbon atoms and CH_3 groups (thin line) in ^{13}C-enriched carbon-SBA-15, ssb=spinning sideband (14 kHz MAS); b) structural model reproducing the experimental spectra. Adapted from ref. [59].

3.4. Deposition of oxide nanoparticles on a carbon support

Recently, we systematically investigated the hydrothermal stability of niobia/carbon composites in aqueous phase reactions conducted at elevated temperatures (≥ 200 °C). Because bulk amorphous niobia lost surface area due to formation of large faceted crystallites, we developed a simple, one-pot synthesis to generate niobia/carbon composites by a deposition precipitation-carbonization (DPC) method (Fig. 11).[75] This preparation method is simpler than the conventional impregnation route which would require acid treatment of the carbon to generate functional groups that are necessary for the stabilization of the deposited oxide. The catalysts generated by the DPC method contained highly dispersed niobia with nanoparticles having an average size of ca. 8 nm. The niobia/carbon composites showed improved hydrothermal stability and higher reactivity for aqueous-phase dehydration of butanol compared to amorphous niobia (HY-340 from CBMM). Embedding niobia in carbon helps prevent the growth in oxide crystallite size due to a strong interaction between niobia and carbon.

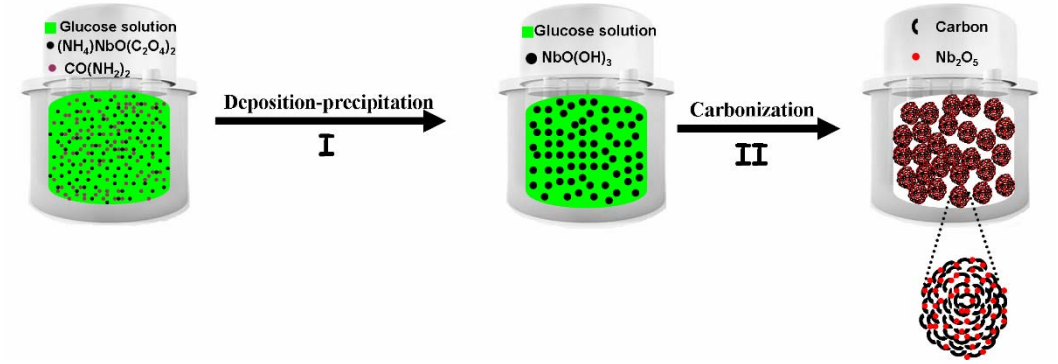

Fig. 11. Preparation of highly dispersed niobia/carbon catalyst by deposition precipitation-carbonization method.[75] Reprinted from Journal of Catalysis, 302, Haifeng Xiong, Hien N. Pham, Abhaya K. Datye, A facile approach for the synthesis of niobia/carbon composites having improved hydrothermal stability for aqueous-phase reactions, 93-100, Copyright (2014), with permission from Elsevier.

.

We also investigated the properties of niobia supported on carbon (carbon black and carbon nanotubes) prepared by impregnation and deposition precipitation (DP) in the aqueous phase.[76] It was found that at 15 atm and 200 °C, large niobia particles were formed due to crystallization on

Green Chemistry Accepted Manuscript

niobia/carbon composites prepared by impregnation. In contrast, no large particles were formed on niobia/carbon composites prepared by DP. The differences between impregnation and the DP method were related to the different pH during deposition of the niobia. The Nb precursor solution is acidic to start with and the niobia species likely remain in the aqueous phase until they reach the solubility limit, causing the formation of weakly bond precipitates. For the DP method, the pH slowly increases as urea decomposes, allowing the niobium hydroxides to preferentially adsorb (and remain adsorbed) on the negatively charged surface. Thus, enhanced interaction was created between the oxide and carbon for the niobia/carbon prepared by DP.

4. Summary

Hydrothermal environments are encountered during the conversion of biorenewables, such as during bio-oil upgrading, bio-diesel production and aqueous phase reforming. The heterogeneous catalysts used for these reactions are subjected to corrosive conditions, leading to poor hydrothermal stability. This review has focused on the major classes of catalysts that have recently been used for these reactions, such as zeolites as well as mesoporous silica- and alumina-based catalysts. Oxide-based materials were found to be unstable under hydrothermal conditions encountered for the majority of biomass conversion reactions. The mechanism of hydrothermal instability in these materials is attributed to Si dissolution and/or Al dissolution from the hydrolysis of Si-O-Si, Al-O-Al or Al-O-Si bonds. We described several approaches to improve the hydrothermal stability of high surface area oxide supports including support surface modification, surface coating of thin-films of oxide or carbon, or through deposition of nanophase oxides on carbon supports. We also note that carbon supports such as carbon black, ordered mesoporous carbon, carbon spheres and carbon nanotubes are generally hydrothermally stable supports in aqueous phase at elevated temperatures, even in supercritical water. Our review focused on the physical stability of the supports under hydrothermal conditions. However, there are other factors that lead to loss of activity such as the leaching of the active phase, loss of specific morphology or surface facets, and the formation of carbonaceous deposits such as coke as well as sintering and oxidation of the metal phase. In summary, hydrothermal stability is an important characteristic for reactions conducted in the aqueous phase and must be considered when designing catalysts for conversion of biorenewables.

Acknowledgements

This work is supported by the NSF Engineering Research Center for Biorenewable Chemicals (CBiRC) supported by NSF grant EEC-0813570. Partial support from NSF grant OISE 0730277 is also gratefully acknowledged.

References

1. R. D. Cortright, R. R. Davda and J. A. Dumesic, *Nature*, 2002, 418, 964-967.
2. J. N. Chheda, G. W. Huber and J. A. Dumesic, *Angew Chem Int Ed Engl*, 2007, 46, 7164-7183.
3. A. A. Peterson, F. Vogel, R. P. Lachance, M. Froling, J. M. J. Antal and J. W. Tester, *Energy & Environmental Science*, 2008, 1, 32-65.
4. H. Weingärtner and E. U. Franck, *Angewandte Chemie International Edition*, 2005, 44, 2672-2692.
5. T. M. Yeh, J. G. Dickinson, A. Franck, S. Linic, L. T. Thompson and P. E. Savage, *Journal of Chemical Technology & Biotechnology*, 2013, 88, 13-24.
6. M. Kögel, V. H. Sandoval, W. Schwieger, A. Tissler and T. Turek, *Chemical Engineering & Technology*, 1998, 21, 655-658.
7. B. R. Johnson, N. L. Canfield, D. N. Tran, R. A. Dagle, X. S. Li, J. D. Holladay and Y. Wang, *Catalysis Today*, 2007, 120, 54-62.
8. Ji Man Kim and R. Ryoo, *Bulletin of the Korean Chemical Society*, 1996, 17, 66.
9. R. Mokaya, *Chemical Communications*, 2001, 933-934.
10. V. Nichele, M. Signoretto, F. Menegazzo, A. Gallo, V. Dal Santo, G. Cruciani and G. Cerrato, *Applied Catalysis B: Environmental*, 2012, 111–112, 225-232.

Green Chemistry Accepted Manuscript

11. M. Selvaraj, S. Kawi, D. W. Park and C. S. Ha, *The Journal of Physical Chemistry C*, 2009, 113, 7743-7749.
12. K. Cassiers, T. Linssen, M. Mathieu, M. Benjelloun, K. Schrijnemakers, P. Van Der Voort, P. Cool and E. F. Vansant, *Chemistry of Materials*, 2002, 14, 2317-2324.
13. M. H. Zahir, K. Sato, H. Mori, Y. Iwamoto, M. Nomura and S.-i. Nakao, *Journal of the American Ceramic Society*, 2006, 89, 2874-2880.
14. Y.-W. Chen, C.-S. Lin and W.-C. Hsu, *Catalysis Letters*, 1989, 3, 99-102.
15. M. H. Zahir, S. Fujisaki, K. Sato, T. Nagano and Y. Iwamoto, *Desalination and Water Treatment*, 2009, 2, 229-236.
16. W. Zhao, C. Li, P. Lu, Q. Wen, Y. Zhao, X. Zhang, C. Fan and S. Tao, *Environmental Technology*, 2012, 34, 81-90.
17. B. Valle, A. G. Gayubo, A. Alonso, A. T. Aguayo and J. Bilbao, *Applied Catalysis B: Environmental*, 2010, 100, 318-327.
18. B. I. Palella, L. Lisi, R. Pirone, G. Russo and M. Notaro, *Kinet Catal*, 2006, 47, 728-736.
19. N. Wilken, R. Nedyalkova, K. Kamasamudram, J. Li, N. Currier, R. Vedaiyan, A. Yezerets and L. Olsson, *Topics in Catalysis*, 2013, 56, 317-322.
20. W. E. J. van Kooten, J. Kaptein, C. M. van den Bleek and H. P. A. Calis, *Catalysis Letters*, 1999, 63, 227-231.
21. J. Panpranot, U. Toophorm and P. Praserthdam, *J Porous Mater*, 2005, 12, 293-299.
22. A. Konaka, T. Tago, T. Yoshikawa, A. Nakamura and T. Masuda, *Applied Catalysis B: Environmental*, 2014, 146, 267-273.
23. H. Li, B. Shen, X. Wang and S. Shen, *Catalysis Letters*, 2005, 99, 165-169.
24. H. Kwon, Y. Kim, I.-S. Nam, S. Jung and J.-H. Lee, *Topics in Catalysis*, 2010, 53, 439-446.
25. D. Chan, A. Gremminger and O. Deutschmann, *Topics in Catalysis*, 2013, 56, 293-297.
26. G. Wu, S. Li, C. Zhang, T. Wang and J. Gong, *Applied Catalysis B: Environmental*, 2014, 144, 277-285.
27. M. C. Tsai and Y. W. Chen, *Catalysis Letters*, 1990, 6, 225-230.
28. T. Nagano, K. Sato, T. Saitoh and S. Takahashi, *Journal of the Ceramic Society of Japan*, 2009, 117, 832-835.
29. C. H. He, W. M. Zhang and R. Wang, *Acta Phys.-Chim. Sin.*, 1996, 12, 971-975.
30. Y. Li, D. Liu, S. Liu, W. Wang, S. Xie, X. Zhu and L. Xu, *Journal of Natural Gas Chemistry*, 2008, 17, 69-74.
31. X. Du, X. Gao, H. Zhang, X. Li and P. Liu, *Catalysis Communications*, 2013, 35, 17-22.
32. G. Niu, Y. Huang, X. Chen, J. He, Y. Liu and A. He, *Applied Catalysis B: Environmental*, 1999, 21, 63-70.
33. N. R. Burke, D. L. Trimm and R. F. Howe, *Applied Catalysis B: Environmental*, 2003, 46, 97-104.
34. J. M. Kim and R. Ryoo, *Bulletin of the Korean Chemical Society*, 1996, 17, 66-68.
35. R. Igi, T. Yoshioka, Y. H. Ikuhara, Y. Iwamoto and T. Tsuru, *Journal of the American Ceramic Society*, 2008, 91, 2975-2981.
36. T. Tsuru, *Journal of the Japan Petroleum Institute*, 2011, 54, 277-286.
37. A. Onda, T. Ochi and K. Yanagisawa, *Topics in Catalysis*, 2009, 52, 801-807.
38. H. Xiong, T. Wang, B. Shanks and A. Datye, *Catalysis Letters*, 2013, 143, 509-516.
39. Z.-j. Zhang, S.-j. Sui, S. Tan, Q.-w. Wang and C. U. Pittman Jr, *Bioresource Technology*, 2013, 130, 789-792.
40. D. Zhao, J. Feng, Q. Huo, N. Melosh, G. H. Fredrickson, B. F. Chmelka and G. D. Stucky, *Science*, 1998, 279, 548-552.
41. R. A. Pollock, G. Y. Gor, B. R. Walsh, J. Fry, I. T. Ghampson, Y. B. Melnichenko, H. Kaiser, W. J. DeSisto, M. C. Wheeler and B. G. Frederick, *The Journal of Physical Chemistry C*, 2012, 116, 22802-22814.
42. M. C. Burleigh, M. A. Markowitz, S. Jayasundera, M. S. Spector, C. W. Thomas and B. P. Gaber, *The Journal of Physical Chemistry B*, 2003, 107, 12628-12634.
43. I. Agirrezabal-Telleria, J. Requies, M. B. Güemez and P. L. Arias, *Applied Catalysis B: Environmental*, 2014, 145, 34-42.
44. J. S. Kruger, V. Nikolakis and D. G. Vlachos, *Applied Catalysis A: General*, 2014, 469, 116-123.
45. P. A. Zapata, J. Faria, M. P. Ruiz, R. E. Jentoft and D. E. Resasco, *Journal of the American Chemical Society*, 2012, 134, 8570-8578.

Green Chemistry Accepted Manuscript

46. M. Moliner, Y. Román-Leshkov and M. E. Davis, *Proceedings of the National Academy of Sciences*, 2010, 107, 6164-6168.
47. Z. Wu, S. Ge, C. Ren, M. Zhang, A. Yip and C. Xu, *Green Chemistry*, 2012, 14, 3336-3343.
48. I. Agirrezabal-Telleria, J. Requies, M. B. Güemez and P. L. Arias, *Applied Catalysis B: Environmental*, 2012, 115–116, 169-178.
49. M. H. Tucker, A. J. Crisci, B. N. Wigington, N. Phadke, R. Alamillo, J. Zhang, S. L. Scott and J. A. Dumesic, *ACS Catalysis*, 2012, 2, 1865-1876.
50. J. Liu, Q. Yang, M. P. Kapoor, N. Setoyama, S. Inagaki, J. Yang and L. Zhang, *The Journal of Physical Chemistry B*, 2005, 109, 12250-12256.
51. A. Onda, T. Ochi and K. Yanagisawa, *Green Chemistry*, 2008, 10, 1033-1037.
52. A. Onda, *Journal of the Japan Petroleum Institute*, 2012, 55, 73.
53. P. P. Upare, J.-W. Yoon, M. Y. Kim, H.-Y. Kang, D. W. Hwang, Y. K. Hwang, H. H. Kung and J.-S. Chang, *Green Chemistry*, 2013, 15, 2935-2943.
54. K. Nakajima, Y. Baba, R. Noma, M. Kitano, J. N. Kondo, S. Hayashi and M. Hara, *Journal of the American Chemical Society*, 2011, 133, 4224-4227.
55. K. Yan, X. Wu, X. An and X. Xie, *Chemical Engineering Communications*, 2013, 201, 456-465.
56. J. Tian, J. Wang, S. Zhao, C. Jiang, X. Zhang and X. Wang, *Cellulose*, 2010, 17, 587-594.
57. J. M. Anderson, R. L. Johnson, K. Schmidt-Rohr and B. H. Shanks, *Catalysis Communications*, 2014, 51, 33-36.
58. C. Liu, S. Lee, D. Su, B. Lee, S. Lee, R. E. Winans, C. Yin, S. Vajda, L. Pfefferle and G. L. Haller, *Langmuir*, 2012, 28, 17159-17167.
59. H. N. Pham, A. E. Anderson, R. L. Johnson, K. Schmidt-Rohr and A. K. Datye, *Angewandte Chemie International Edition*, 2012, 51, 13163-13167.
60. R. M. Ravenelle, J. R. Copeland, W.-G. Kim, J. C. Crittenden and C. Sievers, *ACS Catalysis*, 2011, 1, 552-561.
61. N. Luo, X. Fu, F. Cao, T. Xiao and P. P. Edwards, *Fuel*, 2008, 87, 3483-3489.
62. K. Lehnert and P. Claus, *Catal. Commun.*, 2008, 9, 2543-2546.
63. K. Koichumanova, A. K. K. Vikla, D. J. M. de Vlieger, K. Seshan, B. L. Mojet and L. Lefferts, *ChemSusChem*, 2013, 6, 1717-1723.
64. A. L. Jongerius, J. R. Copeland, G. S. Foo, J. P. Hofmann, P. C. A. Bruijnincx, C. Sievers and B. M. Weckhuysen, *ACS Catalysis*, 2013, 3, 464-473.
65. L. Yang, K. Seshan and Y. Li, *Catalysis Communications*, 2013, 30, 36-39.
66. R. M. Ravenelle, F. Schüβler, A. D'Amico, N. Danilina, J. A. van Bokhoven, J. A. Lercher, C. W. Jones and C. Sievers, *The Journal of Physical Chemistry C*, 2010, 114, 19582-19595.
67. M. W. Hahn, J. R. Copeland, A. H. van Pelt and C. Sievers, *ChemSusChem*, 2013, 6, 2304-2315.
68. L. Vilcocq, A. Cabiac, C. Especel, S. Lacombe and D. Duprez, *Catalysis Communications*, 2011, 15, 18-22.
69. R. M. West, D. J. Braden and J. A. Dumesic, *Journal of Catalysis*, 2009, 262, 134-143.
70. H. N. Pham, Y. J. Pagan-Torres, J. C. Serrano-Ruiz, D. Wang, J. A. Dumesic and A. K. Datye, *Applied Catalysis A: General*, 2011, 397, 153-162.
71. Y. J. Pagán-Torres, J. M. R. Gallo, D. Wang, H. N. Pham, J. A. Libera, C. L. Marshall, J. W. Elam, A. K. Datye and J. A. Dumesic, *ACS Catalysis*, 2011, 1, 1234-1245.
72. Y. T. Kim, J. A. Dumesic and G. W. Huber, *Journal of Catalysis*, 2013, 304, 72-85.
73. H.-D. Kim, T.-W. Kim, H. J. Park, K.-E. Jeong, H.-J. Chae, S.-Y. Jeong, C.-H. Lee and C.-U. Kim, *International Journal of Hydrogen Energy*, 2012, 37, 12187-12197.
74. T.-W. Kim, H.-D. Kim, K.-E. Jeong, H.-J. Chae, S.-Y. Jeong, C.-H. Lee and C.-U. Kim, *Green Chemistry*, 2011, 13, 1718-1728.
75. H. Xiong, H. N. Pham and A. K. Datye, *Journal of Catalysis*, 2013, 302, 93-100.
76. H. Xiong, M. Nolan, B. H. Shanks and A. K. Datye, *Applied Catalysis A: General*, 2014, 471, 165-174.
77. D. J. M. de Vlieger, B. L. Mojet, L. Lefferts and K. Seshan, *Journal of Catalysis*, 2012, 292, 239-245.
78. D. J. M. de Vlieger, A. G. Chakinala, L. Lefferts, S. R. A. Kersten, K. Seshan and D. W. F. Brilman, *Applied Catalysis B: Environmental*, 2012, 111–112, 536-544.
79. A. Wawrzetz, B. Peng, A. Hrabar, A. Jentys, A. A. Lemonidou and J. A. Lercher, *J. Catal.*, 2010, 269, 411-420.

Green Chemistry Accepted Manuscript

80. D. C. Elliott, L. J. Sealock and E. G. Baker, *Industrial & Engineering Chemistry Research*, 1993, 32, 1542-1548.
81. A. G. Chakinala, J. K. Chinthaginjala, K. Seshan, W. P. M. van Swaaij, S. R. A. Kersten and D. W. F. Brilman, *Catalysis Today*, 2012, 195, 83-92.
82. S. Rabe, M. Nachtegaal, T. Ulrich and F. Vogel, *Angewandte Chemie International Edition*, 2010, 49, 6434-6437.
83. D. J. M. de Vlieger, D. B. Thakur, L. Lefferts and K. Seshan, *ChemCatChem*, 2012, 4, 2068-2074.
84. Y. F. Li, J. Q. Zhu, H. Liu, P. Wang and H. P. Tian, *Acta Phys.-Chim. Sin.*, 2011, 27, 52-58.
85. Y. Han, N. Li, L. Zhao, D. Li, X. Xu, S. Wu, Y. Di, C. Li, Y. Zou, Y. Yu and F.-S. Xiao, *The Journal of Physical Chemistry B*, 2003, 107, 7551-7556.
86. R. Mokaya, *The Journal of Physical Chemistry B*, 2000, 104, 8279-8286.
87. J. Wei, J. Shi, H. Pan, Q. Su, J. Zhu and Y. Shi, *Microporous and Mesoporous Materials*, 2009, 117, 596-602.

Green Chemistry Accepted Manuscript